Journal of Non-Crystalline Solids 449 (2016) 100–106

Contents lists available at ScienceDirect

Journal of Non-Crystalline Solids

journal homepage: www.elsevier.com/locate/jnoncrysol

Molecular dynamics simulations of pressure-induced structural and mechanical property changes in amorphous Al_2O_3

Giang T. Nguyen [a], Thao T. Nguyen [a,b], Trang T. Nguyen [a], Vinh V. Le [a,*]

[a] Department of Computational Physics, Hanoi University of Science and Technology, Hanoi, Vietnam
[b] Faculty of Physics, Hanoi National University of Education, Hanoi, Vietnam

ARTICLE INFO

Article history:
Received 25 May 2016
Received in revised form 5 July 2016
Accepted 14 July 2016
Available online 22 July 2016

Keywords:
Molecular dynamics
Amorphous alumina
Units AlO_x
Crystalline
Mechanical properties

ABSTRACT

Molecular dynamics (MD) simulations of amorphous alumina have been carried out to investigate the pressure-induced structural transformation and mechanical properties. We found that not only the fraction of units AlO_x ($x = 4, 5, 6$) but also the density of each AlO_x type change upon compression. The density of sample can be expressed through the fraction and partial density of units AlO_x. With increasing pressure, O atoms are more ordered than Al atoms and form fcc and hcp clusters. The same units AlO_x link together to form atomic clusters (AC) of type AC_4, AC_5 and AC_6 (AC_4, AC_5 and AC_6 consist of units AlO_4, AlO_5 and AlO_6, respectively). The Young's modulus can also be expressed through the fraction and partial Young's modulus of units AlO_x.

1. Introduction

Amorphous alumina (a-Al_2O_3) has been being materials of great technological applications such as a high-*k* dielectric [1], in optical devices [2], luminescence [3], catalysis [4], corrosion and wear-resistant [5]. Although prototypical Al_2O_3 alone cannot be obtained as a bulk glass [6], however, a-Al_2O_3 can be produced as thin film through anodic process [7–10] or vapor deposition [11–18]. Nanoparticles of a-Al_2O_3 have also synthesized by the laser evaporation process [19]. The structure of a-Al_2O_3 contains basic units AlO_x ($x = 4$, 5 and 6) network. The network topology of a-Al_2O_3 have been analyzed experimentally using extended X-ray absorption fine structures (EXAFS) [7], electron extended energy loss fine structure (EXELFS) [8], X-ray and neutron diffraction [9,10], and solid-state NMR experiments [14–16,19]. In these studies, only the first two diffraction peaks of the crystalline solid remain with the Al—O bond length varied from 1.8 Å to 1.9 Å and different ratios of AlO_x units. Furthermore, these experiments have confirmed that the density of a-Al_2O_3 varies over a large range, between 2.1 and 3.8 $g \cdot cm^{-3}$ [6–8], which implies the existence of many metastable states. However, in our best knowledge, no experimental evidence of the polyamorphism [20] in pure a-Al_2O_3 has been presented yet, such as Ge_2O [21], SiO_2 [22] and Y_2O_3-Al_2O_3 [23] glasses which have two distinct amorphous states, denoted high-density amorphous (HDA) and low-density amorphous (LDA). Although molecular dynamics (MD) simulations [24–29] have showed that the existence of structural transformation from a tetrahedral to an octahedral network structure upon compression, no evidence of a first – order phase transition has observed in a-Al_2O_3. These simulations imply that the LDA phase contains units AlO_4 and the HDA phase may contain units AlO_5 and AlO_6, but the density of each separate kind of units AlO_x has not been presented. The same units AlO_x ($x = 4$ or 5 or 6) may be located nearby via common oxygen and create atomic clusters (AC). Consequently, there are three types of ACs in the network structure: AC_4, AC_5 and AC_6 which consist of AlO_4, AlO_5 and AlO_6 units, respectively. Not only there is no report on the distribution of the ACs but also the mechanical behavior of the each AC_x ($x = 4$ or 5 or 6) upon compression have not been investigated yet. Furthermore, upon compression, the pair radial distribution function (RDF) $g_{O\text{-}O}(r)$ has showed more structural peaks [25,26] which imply the significant change of the intermediate range order in a-Al_2O_3 samples. Therefore, in this work, we report on the results of density and the structural evolution of a-Al_2O_3 under compression, and discuss the AC_x and mechanical behavior of these systems.

2. Computational procedures

The MD simulation has been performed using a configuration containing 5000 atoms (2000 Al and 3000 O) in a cube under periodic boundary conditions. We apply the Coulomb-Buckingham potential which correctly produces the liquid and amorphous structures [23,30]. The long-range Coulomb interactions were calculated with the Ewald summation technique, which is applied to three-dimensional periodic boundary conditions. The Verlet algorithm with a time step of 1 fs is adopted and the simulation was executed at a constant pressure (the ensemble NPT). The initial configuration was randomly generated all atoms in the simulation box corresponding to the density of

* Corresponding author.
E-mail address: vinh.levan@hust.edu.vn (V.V. Le).

http://dx.doi.org/10.1016/j.jnoncrysol.2016.07.018
0022-3093/

2.8 g.cm^{-3} with condition that no two atoms be closer than 1.0 Å. This sample was heated at the temperature of 5000 K and the pressure of 0 GPa for over 5×10^5 time steps and subsequently cooled down to 300 K at 1 K/ps. At 300 K, relaxation was performed over 10^5 time steps without any disturbance. Other samples were obtained by the compression procedure with different pressure. The simulation was performed as follows: the sample at the pressure of 0 GPa is compressed to pressure P for 10^6 time steps and then relaxed for over 10^5 time steps. The obtained sample is in the completed equilibrium.

In order to determine the structural unit AlO_x we used the cut-off distances, usually chosen as the position of the minimum after the first peak of the pair RDFs $g_{Al\text{-}O}(r)$. To calculate the void, the radius of Al and O atoms is 1.23 and 0.73 Å, respectively. The void is defined as a sphere that can be inserted in contact with four atoms and do not intersect with any atom. Strain-stress simulations with a strain rate of 2×10^{11} s^{-1} were calculated following the computational procedures which were described in detail elsewhere [29].

3. Results and discussion

We obtain the Al_2O_3 samples with the volume and density dependence of the pressure as displayed in Fig. 1. We can see that the volume decreases drastically with increasing pressure from 0 to 25 GPa and then gradually with a further increase of pressure. This P-V isotherm shows that no discontinuous changes like the first-order transition in H_2O [31] or SiO_2 [32] glasses, and this result is good agreement with one in Ref. [26]. At the pressure of 0 GPa, the density is 2.93 g·cm^{-3}, and this value is little higher than that in the work [26,28] but little lower than that in Ref. [25]. Possibly, it is related to different potentials used here and in Refs. [25,26,28]. However, Skinner et al. [33] reported that the model of Al_2O_3 used the partial charges potential [30] gives not only consistent density with the most recent density measurements, but also the best overall agreement with the diffraction data. This is a reason why, therefore, the partial charges potential [30] was used in this work. With increasing pressure from 0 to 25 GPa, the density increases greatly and then almost linearly gradually with a further increase of pressure. Here we found that density increases ~20% at $P =$ 20 GPa while it increases ~22% at $P = 20$ GPa [26] and ~14% at $P =$ 25 GPa [28]. Although there is no experiment of the pressure-induced structural transformation in a-Al_2O_3, however, both experiment [34] and first-principles computations [35] show that the transformation from corundum to Rh2O3(II)-type alumina at 87–113 GPa occurs with the increase of density ~34%. More theoretical [36] and experimental [37–39] pressure-volume isotherms of corundum have been performed. With increasing pressure from 0 to 10 GPa, the volume of a-Al_2O_3 varies faster than that of corundum, but the varied volume in both of a-Al_2O_3 and corundum is almost similarly with further increase of the pressure.

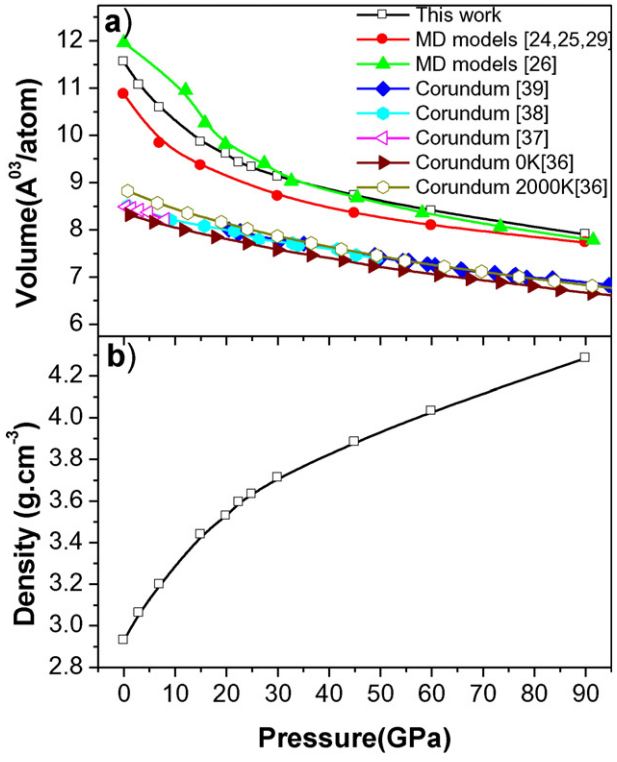

Fig. 1. a) Pressure-volume isotherms of a-Al_2O_3 and corundum, and b) density dependence of the pressure of a-Al_2O_3 systems at the temperature of 300 K.

Fig. 2 displays the total RDFs for neutron scattering $G_N(r)$ and pair RDFs of Al_2O_3 samples. For the total RDFs $G_N(r)$ exhibiting the short-order structure of amorphous phase (see Fig. 2a), the first peak shifts to the right from 1.80 to 1.82 Å, while the second peak shifts to the left from 2.86 Å to 2.54 Å with increasing pressure. At the density of 3.20 g·cm^{-3} ($P =$ 7GPa), the $G_N(r)$ of the model is good agreement with the experimental data [10,40]. The first peak of the $G_N(r)$ is contributed from the pair RDF $G_{Al\text{-}O}(r)$ and the second peak is contributed from the pair RDFs $G_{Al\text{-}Al}(r)$ and $G_{O\text{-}O}(r)$. For the $G_{Al\text{-}O}(r)$ exhibiting the Al—O bond distance (see Fig. 2b), the shape is almost unchanged except the height and position of the first peak with increasing pressure. Fig. 2c shows the $G_{Al\text{-}Al}(r)$ in that the first peak is broadening and shifts to the left from 3.20 Å to 2.80 Å upon compression. The first peak of the $G_{O\text{-}O}(r)$ (see Fig. 2d) also shifts to the left from 2.82 to 2.54 Å, but a new peak appears at the position of 3.68 ± 0.06 Å with increasing pressure above 15 GPa. These new peaks were also observed in other simulations upon compression of a-Al_2O_3 [25,26] but no clear explain has been provided yet. They like the second peak of crystalline structure (faced centered cubic – fcc or hexagonal closed packed – hcp). There is experimental evidence indicating that the structural ordering of the distorted oxygen (O) sublattice is associated with a densification of the Al_2O_3 film due to the reduction of free volume [41]. This experiment also confirms that, during the amorphous to crystalline transition, no considerable short-range ordering or redistribution of Al cations over AlO_4 or AlO_6 interstices of the distorted, densely packed O sublattice, occurs. Recently, C. Kong et al. used classical MD simulations [42] presented that the crystallization of vitreous Al_2O_3 includes the O atoms packed in fcc structure and the Al atoms randomly located in space. Here we used the common neighbor analysis (CNA) [43] to examine the structure of a-Al_2O_3 samples. We found that only the O atoms arrange in both fcc and hcp lattices and do not possess icosahedral order with increasing pressure above 7 GPa. Under compression, these O atoms grow in the form of fcc and hcp clusters, in that they contain a few ten atoms as presented in Fig. 3. Our results also indicate that hcp order is more little favorable than fcc, because the former allows more fluctuations in the structure [44]. Furthermore, this may be related to the softer nature of hcp than for fcc against some deformation modes [45]. Let N_{Crys} be the number of fcc and hcp atoms, and N_O be the number of O atoms in the sample. At the pressure of 7 GPa, the ratio N_{Crys}/N_O is 0.02 in the sample. This ratio increases with increasing pressure and reaches 0.195 at the pressure of 90 GPa. The O atoms of crystalline clusters distributed over units AlO_x ($x = 4, 5$ and 6) are presented in Table 1. We realize that the distribution of these O atoms over units AlO_x strongly depends on the compression, due to the fraction of units AlO_x changed with increasing pressure (see Fig. 4a). The Al atoms, the nearest-neighbor crystalline O atoms, randomly distribute over units AlO_x not only in fcc O clusters but also in hcp O clusters. Therefore, the here observed fcc O clusters is further denoted as the nucleation sites of γ″-Al_2O_3 in the literature [46] and observed hcp O clusters denoted as the nucleation sites of k′-Al_2O_3 in the literature [47]. We also calculated the contribution to the new peak of the $G_{O\text{-}O}(r)$ (at the position of 3.68 ± 0.06 Å) from the fcc and hcp O clusters, in that they contribute ~8% at the pressure of 30 GPa and ~30% at the pressure of 90 GPa.